Quantification of spread of cerebellar long-term depression with chemical two-photon uncaging of glutamate

Samuel S.-H. Wang*, Leonard Khiroug, and George J. Augustine†

Department of Neurobiology, Duke University Medical Center, Box 3209, Durham, NC 27710

Edited by Charles F. Stevens, The Salk Institute for Biological Studies, La Jolla, CA, and approved May 3, 2000 (received for review September 27, 1999)

Localized, chemical two-photon photolysis of caged glutamate was used to map the changes in α-amino-3-hydroxy-5-methyl-4-isoxazolepropionic acid-type glutamate receptors caused by long-term synaptic depression (LTD) in cerebellar Purkinje cells. LTD produced by pairing parallel fiber activity with depolarization was accompanied by a decline in the response of Purkinje cells to uncaged glutamate that accounted for both the time course and magnitude of LTD. This depression of glutamate responses was observed not only at the site of parallel fiber stimulation but also at more distant sites. The amount of LTD decreased with distance and was half-maximal 50 μm away from the site of parallel fiber activity. Estimation of the number of parallel fibers active during LTD induction indicates that LTD modified glutamate receptors not only at active synapses but also at 600 times as many inactive synapses on a single Purkinje cell. Therefore, both active and inactive parallel fiber synapses can undergo changes at a postsynaptic locus as a result of associative pre- and postsynaptic activity.

synaptic plasticity | glutamate receptors | calcium | flash photolysis

Use-dependent synaptic plasticity has been proposed to serve as a mechanism for storing information in the brain (1–3). One fundamental question regarding this hypothesis is the location of the synapses that are modified. Although it has been widely assumed that individual synapses represent storage sites (2), there are now several cases where plasticity appears to extend beyond individual synapses (4–8).

Here we examine the spatial range of cerebellar long-term depression (LTD), a form of plasticity that has been implicated in motor learning (9–12). LTD is associative because it arises from the coincident activity of parallel fiber (PF) and climbing fiber synapses onto Purkinje cells (9, 13–15). The precise range of action of LTD is not yet clear. Although LTD is thought to occur only at PFs that are active during LTD induction (16–18), a nonassociative form of LTD has been reported to spread more than 100 μm (18). Two unique features make it possible for us to define the range of cerebellar LTD. (*i*) The organized geometry of PF axons allows selective activation of PF synapses in a defined area. (*ii*) LTD is thought to arise from a change in the sensitivity of postsynaptic, α-amino-3-hydroxy-5-methyl-4-isoxazolepropionic acid (AMPA)-type glutamate receptors (13, 19, 20), allowing these receptors to serve as a read-out for the spread of LTD. By using chemical two-photon uncaging of glutamate (21) to monitor the properties of AMPA receptors, we have found that LTD affects glutamate receptors over a range of up to 60 μm. Because the region of PF activation is ≈10 μm, these results show that LTD stores information both at active PF synapses and at nearby inactive PF synapses. This spread of LTD requires a chemical signal that can move from active to inactive PF synapses on the same Purkinje cell.

Materials and Methods

Patch Clamp Recordings. Whole-cell patch clamp recordings were made from Purkinje cells as described previously (22, 23). Sagittal slices were cut from cerebella of 12- to 21-day-old rats and bathed in extracellular solution containing 119 mM NaCl, 2.5 mM KCl, 1.3 mM Mg_2SO_4, 2.5 mM $CaCl_2$, 1.0 mM NaH_2PO_4, 26.2 mM $NaHCO_3$, 10 mM glucose, 0.05–0.1 mM Trolox C, and 0.01 mM bicuculline methiodide. All reagents were obtained from Sigma, except for 6-cyano-7-nitroquinoxaline-2,3-dione (CNQX; Research Biochemicals, Natick, NYI); Trolox C (Fluka); and γ-carboxynitrobenzyl (CNB)-glutamate, α,γ-bis-CNB-glutamate, 1,2-bis(2-aminophenoxy)-ethane-*N*,*N*,*N*′,*N*′-tetraacetic acid (BAPTA), and Oregon Green 488 BAPTA-1 (Molecular Probes). Patch electrodes were filled with a solution containing 130 mM potassium gluconate, 2 mM NaCl, 4 mM Na_2ATP, 0.4 mM NaGTP, 4 mM $MgCl_2$, and 20 mM Hepes (pH 7.3). Pipettes contained Oregon Green 488 BAPTA-1 (0.2–0.5 mM) unless otherwise indicated. Pipette resistances were 3–4 MΩ; access resistances were 8–20 MΩ and varied by <15% in experiments described here. Cells were voltage clamped at −60 mV with no junction potential or series resistance correction, and data were sampled at 4 kHz. Parallel fibers were stimulated with a saline-filled glass pipette placed in the molecular layer with its tip 10–30 μm above the dendritic arbor of the Purkinje cell. After recording PF responses and caged glutamate responses for at least 10 min, LTD was induced by pairing PF stimuli with 50-ms depolarizations to 0 mV, 50–200 times at 1 Hz. Currents were analyzed with CLAMPFIT software (Axon Instruments, Foster City, CA), and statistical significance was tested by using Student's one-tailed *t* test unless otherwise indicated.

Optical Methods. Photolysis of caged glutamate and calcium imaging and were performed on a confocal microscope (Noran Odyssey) as described previously (21, 24). Double-caged glutamate [α,γ-bis-(α-carboxynitrobenzyl)-glutamic acid] or, occasionally, single-caged glutamate [γ-(α-carboxynitrobenzyl)-glutamic acid] was added to the saline and uncaged via a spot of UV light 3–5 μm in width (24). Light flashes were 2–10 ms in duration and contained 2–10 μJ of energy. To identify the region of PF activation, stimulus trains (10 pulses, 50 Hz) were used to activate large local Ca signals that were measured by Oregon Green BAPTA-1 (18, 25, 26). Calcium images were analyzed with MATLAB (MathWorks) and Scion Image (Scion). Fluorescence signals were corrected for background and displayed as

This paper was submitted directly (Track II) to the PNAS office.

Abbreviations: AMPA, α-amino-3-hydroxy-5-methyl-4-isoxazolepropionic acid; BAPTA, 1,2-bis(2-aminophenoxy)-ethane-*N*,*N*,*N*′,*N*′-tetraacetic acid; CNB, carboxynitrobenzyl; CNQX, 6-cyano-7-nitroquinoxaline-2,3-dione; LTD, long-term depression; PF, parallel fiber; SVD, singular value decomposition; EPSP, excitatory postsynaptic potential.

*Present address: Department of Molecular Biology, Princeton University, Princeton, NJ 08544.

†To whom reprint requests should be addressed. E-mail: georgea@neuro.duke.edu.

The publication costs of this article were defrayed in part by page charge payment. This article must therefore be hereby marked "*advertisement*" in accordance with 18 U.S.C. §1734 solely to indicate this fact.

Article published online before print: *Proc. Natl. Acad. Sci. USA*, 10.1073/pnas.130414597. Article and publication date are at www.pnas.org/cgi/doi/10.1073/pnas.130414597

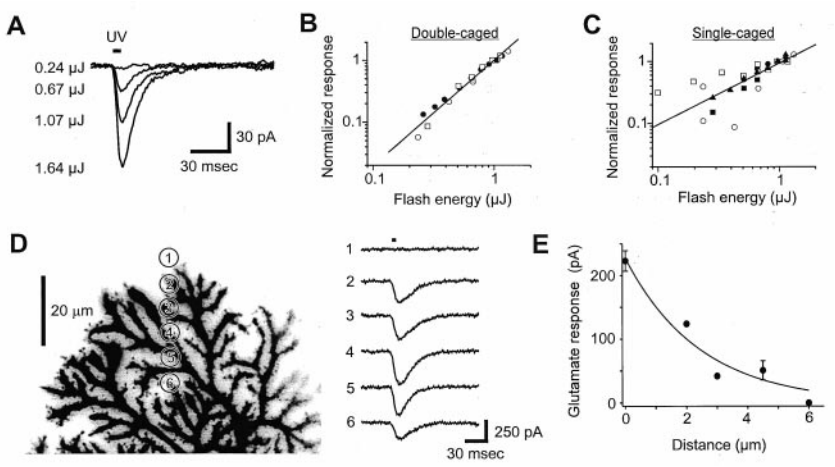

Fig. 1. Nonlinear and localized activation of glutamate receptors by chemical two-photon uncaging. (*A*) Current responses to single-caged glutamate photolyzed by 6-ms UV flashes (at bar) of varying intensities focused on the soma of a Purkinje neuron. (*B* and *C*) Relationships between peak inward currents and light flash energy for double-caged (*B*) and single-caged (*C*) glutamate. Responses are normalized to the responses measured at 1 μJ. Each symbol represents a different cell. Least-squares fits to the data are shown by lines, with slopes of 1.7 in *B* and 1.0 in *C*. (*D Left*) Glutamate was produced by moving the uncaging spot to the locations indicated by numbered circles. This Purkinje cell was filled with Oregon Green 488 BAPTA-1 and contrast on this and all other fluorescence images in this paper is reversed, so that fluorescence is dark. (*D Right*) Responses elicited by uncaging glutamate (bar) at the locations shown (*left*). (*E*) Relationship between glutamate response and position of the UV light spot beyond the end of a Purkinje cell dendrite. Error bars indicate the SEM for points that represent the means of several measurements (n = 14 for 0 μm; n = 2 for 4.5 μm). Curve is an exponentially decaying function with a length constant of 2.4 μm.

$\Delta F_{max}/F_0$, the maximum fractional change in dye fluorescence. The region of elevated Ca was identified by using singular value decomposition (SVD), also known as principal component analysis (27). In SVD, a time series stack of images is separated into a linear combination of orthogonal response modes. This approach sensitively detects temporally correlated activity shared among different pixels and is resistant to noise-based fluctuations relative to simpler measures such as $\Delta F/F_0$ (28). Image stacks were averaged to a pixel size of 2 μm, and the mean intensity of the entire stack was subtracted. In all experiments, SVD on this signal revealed exactly one response mode, with higher-order modes corresponding to noise, as determined by the "scree" test (27). Pixels were defined as responding if their response mode amplitude was greater than 1 SD.

Results

Chemical Two-Photon Activation of Glutamate Receptors in Purkinje Cells. We began by characterizing the ability of local photolysis of caged glutamate (21, 29) to activate glutamate receptors on Purkinje cells. Glutamate was generated by a 3- to 5-μm diameter UV light spot, which produced inward currents within 0.4 ± 0.1 ms (SEM, 34 sites in 7 cells) of the beginning of the light flash (Fig. 1*A*). CNQX, a competitive antagonist that blocks AMPA receptors (30–32), completely and reversibly blocked these currents. Approximately 200 nM CNQX was required to half-maximally block these responses. These results indicate that uncaged glutamate is produced in close proximity to Purkinje cells and activates their AMPA receptors.

We used double-caged glutamate to eliminate glutamate production above and below the focal point of the light beam (21). Two tests confirmed that two photolysis events were necessary to produce free glutamate. First, responses evoked by double-caged glutamate were a nonlinear function of UV light energy. Response amplitude was well fitted by a second-power function of flash energy (Fig. 1*B*; power-law slope n_H = 1.7 ± 0.1, 3 cells). In contrast, responses evoked by single-caged glutamate increased as an approximately linear function of the amount of energy in the light flash (Fig. 1*C*; n_H = 1.0 ± 0.1, 4 cells). This finding indicates that two photons are needed to produce free glutamate from the double-caged glutamate.

The second test was based on measuring the axial range of glutamate uncaging. Defocussed photolysis of single-caged glutamate should yield depth resolution on the order of the diameter of the Purkinje cell arbor (21), ≈100 μm. The observed axial resolution of chemical two-photon uncaging should reflect both the depth (15 μm; ref. 24) of the UV beam waist (21), which is a measure of the true resolution, and the thickness of the Purkinje cell (15–20 μm; ref. 33) as the scanned beam activates receptors on neuronal processes in different focal planes. Axial resolution was determined by varying the axial distance between the Purkinje cell and the focal point of a light spot positioned over the dendrites. The depth of half-maximal glutamate responsiveness was 32 ± 2 μm (n = 16) for double-caged glutamate and 91 ± 23 μm (n = 3) for single-caged glutamate ($P < 0.005$). This improvement in resolution provides further proof of a chemical two-photon effect.

The spatially restricted production of glutamate from the double-caged compound also yields high lateral resolution (34). Glutamate responses were seen only when the light beam was directly over a cell or dendrite; when the uncaging spot was moved 6 μm away from a dendrite there was no response (Fig. 1*D*), with the length constant for glutamate production being less than 3 μm (Fig. 1*E*). This high resolution allowed us to characterize the effects of LTD on AMPA receptors in small regions of the Purkinje cell.

Changes in AMPA Receptor Responses During LTD. LTD was produced by stimulating PF axons in conjunction with depolarization of the Purkinje cell. A small stimulating pipette on the surface of sagittal slices should activate PFs in a very small dendritic area, because PF axons diverge very little and are perpendicular to the surface of such slices (Fig. 2*A*). We performed two measurements to determine precisely where PFs were activated by our stimulating conditions. First, we found that PF responses were essentially undetectable when the pipette was moved, along the slice surface, 10 μm from the edge of a Purkinje cell (Fig. 2 *B–D*). The apparent length constant of the extracellular stimulus was ≈5 μm (Fig. 2*E*). Second, the site of PF activity was localized by using a fluorescent Ca indicator to visualize local Ca signals resulting from PF stimulation (18, 25,

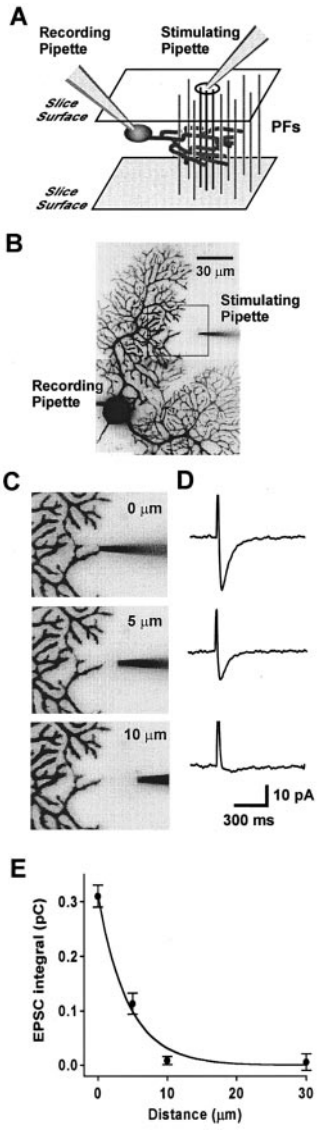

Fig. 2. Restricted range of PF activation by a stimulating pipette. (*A*) Diagram of experimental arrangement. A stimulating pipette was used to activate PFs, which produced excitatory postsynaptic potentials (EPSCs) in Purkinje cells voltage clamped with a recording pipette. (*B*) Volume-rendered fluorescence image of a Purkinje cell, illustrating actual experimental arrangement. Box indicates area shown in *C*. (*C*) Positions of the PF stimulating pipette at the times the recordings shown in *D* were made. (*D*) PF-EPSCs evoked when the stimulating pipette was moved. (*E*) Relationship between PF current integrals and location of the stimulating pipette. Points represent the mean of six separate experiments and bars indicate the SEM.

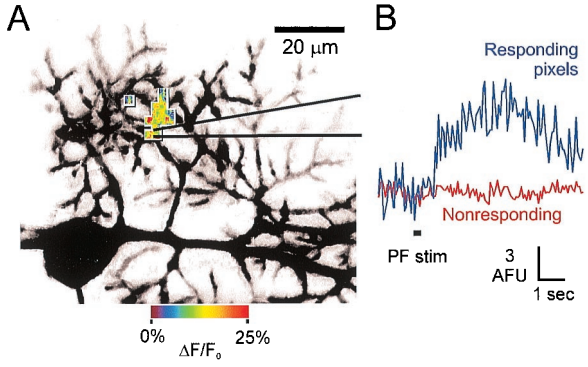

Fig. 3. Range of PF activation assessed by calcium imaging. (*A*) The region of PF activation was identified by SVD analysis of calcium signals produced by a burst of PF activity (10 stimuli, 50 Hz). Differences in the response mode of more than 1 SD above zero were defined as responding (boxed area). The change in fluorescence for responding pixels are indicated in the pseudocolored scale shown at bottom. (*B*) Mean time course of fluorescence changes evoked by the PF stimulus in responding (blue) and nonresponding (red) pixels.

26, 35). PFs were stimulated repetitively (10–16 times at 50 Hz) to evoke maximal Ca increases (26, 35) and provide an upper estimate of the range of PF activity. Calcium transients were analyzed by using SVD, a signal processing technique that extracts with great sensitivity activity patterns shared among pixels in an image stack. SVD analysis showed that the region of PF-induced Ca elevation was confined to a dendritic area 11 ± 4 μm (mean ± SD) in radius that was centered on the stimulating pipette (Fig. 3 *A* and *B*; $n = 3$). In sum, PFs are activated only within a radius of ≈10 μm or less from the stimulating pipette.

Pairing PF activity with depolarization of the Purkinje cell (50–200 times to 0 mV, 50 ms, 1 Hz) caused a LTD of PF-induced synaptic currents (Fig. 4*A*, *Top*), as previously reported (36–38). Before LTD, PF responses ranged from 60 to 360 pA in six cells. In these cells, PF synaptic currents declined from a mean of 146 ± 27 pA to 116 ± 24 pA at 30 min after pairing. The LTD-induced reduction in PF transmission was as great as 33%, with a mean of 20 ± 2% at 30 min following pairing. This LTD was time-dependent and reached a minimum within 30 min (Fig. 4*B*), very similar to LTD resulting from pairing PF and climbing fiber activity (36, 38, 39).

In the same experiments where LTD was induced by pairing PF activity with depolarization, double-caged glutamate was repeatedly photolyzed at the site of PF stimulation to monitor the Purkinje cell AMPA receptors. Although glutamate application was not paired with depolarization (or with PF activity), LTD also caused responses to uncaged glutamate to decline (Fig. 4*A*, *Lower*). When measured 15–30 min after pairing, the amplitude of glutamate responses declined on average by 31 ± 2% ($n = 6$), a value equal to or greater than the reduction of PF responses (one-tailed t test, $P < 0.01$). Like the LTD of PF transmission, the reduction in glutamate response amplitude was time-dependent and developed over tens of minutes (Fig. 4*C*). The effects of LTD on PF and caged glutamate responses were closely matched in time (Fig. 4*D*). Changes in the amplitude of glutamate responses were highly correlated ($r = 0.81$) with the amplitudes of PF synaptic currents measured at the same time points (Fig. 4*E*). PF responses depressed slightly less than glutamate responses, probably because of a superimposed presynaptic enhancement of the PF responses (36, 38, 40).

These parallel declines in both PF synaptic transmission and the response of AMPA receptors to glutamate suggests that LTD affects AMPA receptors. Three results indicated that the decline in responses to uncaged glutamate was associated with LTD rather than a nonspecific run-down. First, glutamate responses decreased by only 6.4 ± 0.9% ($n = 4$) over 30 min in control cells that were not depolarized to avoid inducing LTD (Fig. 5*A*). Glutamate responses decreased significantly more (31 ± 2%; $P < 0.0001$, two-tailed t test) in cells where LTD was induced. This finding shows that glutamate responses decreased only when LTD was induced and that receptor activation by the uncaged glutamate was insufficient to depress AMPA receptors. Second, blocking LTD by including the calcium chelator BAPTA (10 mM) in the patch pipette (38), prevented both LTD of PF transmission and the reduction in glutamate responses (Fig. 5*B*). As reported previously (38), PF responses increased slightly (6 ± 3%; $n = 4$; $P < 0.05$ compared with cells without

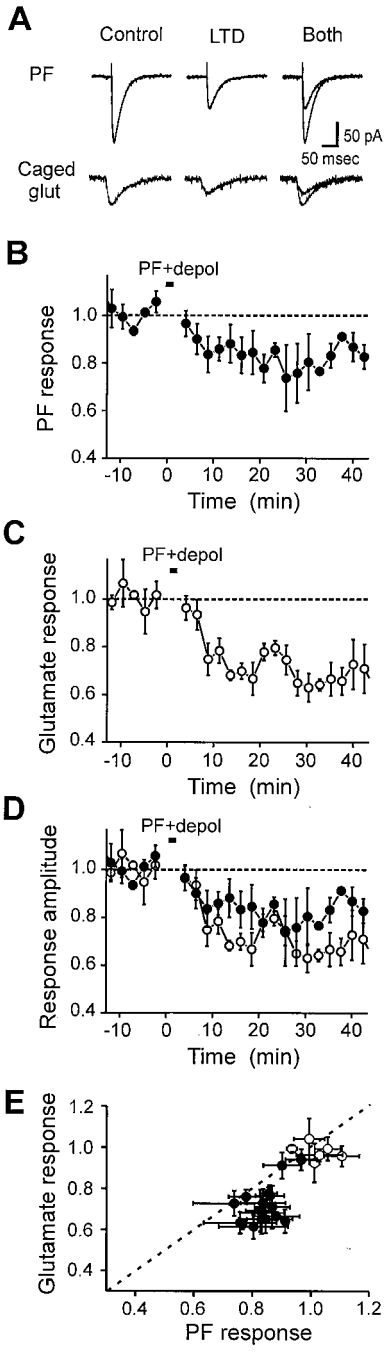

Fig. 4. Changes in postsynaptic receptor sensitivity parallel the LTD of PF transmission. (*A*) PF and caged glutamate responses before (control) and 15 min after LTD was induced (LTD); responses recorded before and after LTD are superimposed at right. Traces are averages of five PF responses or two caged glutamate responses. The uncaging spot was placed within 3 μm of the PF stimulation pipette in this experiment. (*B*) Time course of changes in PF responses during LTD. LTD was induced by pairing PF activity with Purkinje cell depolarization during the time indicated by the horizontal bar. Points represent mean values for peak amplitude of EPSCs measured at the indicated times and bars indicate SEM determined for six experiments. (*C*) Time course of LTD-induced changes in Purkinje cell responses to uncaged glutamate, from the same experiments shown in *B*. Points represent mean amplitudes of glutamate responses and bars indicate SEM. (*D*) Superimposed time courses of LTD-induced changes in responses to PF stimuli (filled symbols) and uncaged glutamate (open symbols). (*E*) Relationship between peak amplitudes of PF and caged glutamate responses. Open symbols indicate responses measured before pairing PF activity with depolarization, and filled symbols indicate responses measured afterward. Dashed line has a slope of 1.

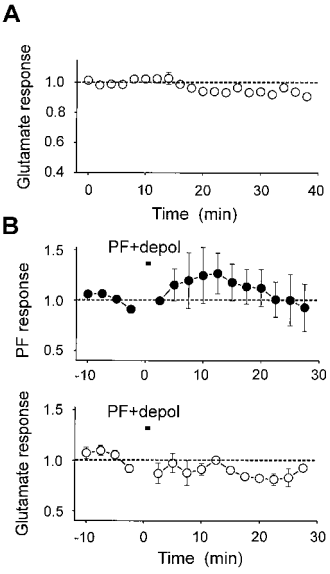

Fig. 5. Mechanisms of depression of glutamate responses. (*A*) Glutamate was uncaged repeatedly at the same location and the amplitude of the responses was virtually unchanged over 40 min, showing that depression is not because of run-down. (*B*) Pairing PF activity with depolarization (horizontal bars) did not depress PF EPSCs (*Upper*) or glutamate responses (*Lower*) in four Purkinje cells filled with BAPTA, demonstrating a requirement for intracellular calcium. Points represent mean values and vertical bars indicate SEM.

BAPTA). LTD of glutamate responses in BAPTA-loaded cells was significantly smaller than that measured without BAPTA ($12 \pm 3\%$ decrease; $n = 4$; $P < 0.005$; decline not significantly greater than change with no pairing, $P = 0.1$). Third, as mentioned above, the LTD-induced changes in PF responses and responses to uncaged glutamate were highly correlated (Fig. 4*E*). Thus, we conclude that LTD affects AMPA receptors and that these changes in postsynaptic AMPA receptors are quantitatively sufficient to account for the changes in synaptic transmission that occur during LTD.

Spatial Range of LTD. To determine where LTD affected AMPA receptors, we positioned the glutamate uncaging spot at variable distances from the pipette that stimulated PF synapses while pairing PF stimuli with depolarization to cause LTD. Although the amount of LTD of the PF responses was similar regardless of location of the UV light spot, the degree of depression of the glutamate responses depended on where the glutamate was photoreleased. When glutamate was produced at the site of PF stimulation, there was a very similar reduction in both glutamate and PF responses (Fig. 6*A*), as described above (Fig. 4 *D* and *E*). However, depression of the glutamate responses was smaller at longer distances from the stimulated PFs, as in the cells shown in Fig. 6 *B* and *C*. This finding indicates that spread of LTD occurred over an area larger than the region of PF stimulation but smaller than the entire Purkinje cell.

To obtain more information about the spatial range of LTD spread, we repeatedly scanned the UV light spot at several locations on the same Purkinje cell while inducing LTD by pairing PF stimuli with depolarization. Under such conditions, repeated photorelease of glutamate at the same location produced responses that varied <10%. Again, LTD was observed to extend well beyond the region of PF activity. In the example shown in Fig. 6 *D* and *E*, AMPA receptors were depressed not only at the site of PF stimulation (site 2) but also in dendritic regions that were beyond the region of PF activity (sites 1 and 3), as indicated both by the absence of a detectable rise in Ca

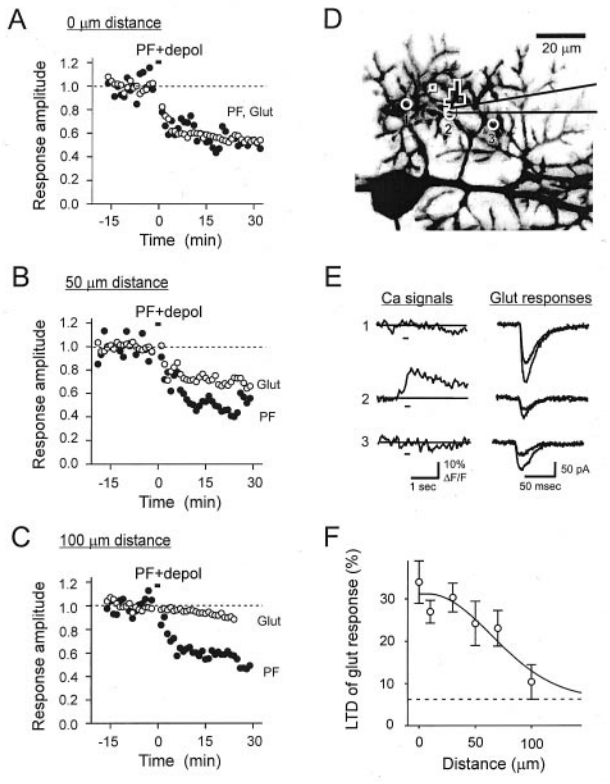

Fig. 6. Long-term depression of AMPA receptors spreads beyond the site of synaptic activity. (*A–C*) Depression of glutamate receptors depends on the distance between the uncaging spot and active PFs. Bars indicate the period of pairing PF activation with depolarization (PF + depol). Filled symbols represent the amplitude of EPSCs resulting from PF activity, whereas open symbols indicate the amplitude of currents produced by uncaging glutamate. When glutamate was uncaged at the same place as the PFs were activated (0 μm, *A*), the glutamate-induced currents depressed but when glutamate was uncaged 100 μm away from the site of PF activity (*C*) there was little depression of these currents. Each panel shows data from a different cell. (*D–E*) Simultaneously monitoring LTD at several sites. (*D*) Diagram of the experiment, showing the same cell used for the singular value decomposition analysis in Fig. 3*E*. (*E Left*) Ca signals recorded at the three sites indicated in *D* during stimulation of PFs (at bars). Only site 2 responded to the focal PF activity. (*E Right*) Following induction of LTD, glutamate responses depressed at all three sites indicated in *D*. (*F*) Superimposed traces are responses (average of 5) recorded 5 min before and 20 min after LTD induction. Relationship between the average decrease in glutamate response, measured 20 min after pairing in 14 cells, and the distance that these responses were elicited from the PF stimulus electrode. Dashed line indicates rate of run-down of glutamate responses in the absence of LTD (Fig. 5*A*) and smooth curve is a Gaussian function with a radius (at half-maximal amplitude) of 56 μm.

during PF stimulation (Fig. 6*E*) and the measured extent of the extracellular stimulus (Fig. 1*E*). Combined results of 14 such experiments, covering a wide spatial range, revealed that the amount of LTD depended on the distance from the site of active PFs (Fig. 6*F*). Glutamate responses <40 μm from the site of PF stimulation were depressed the most, whereas responses were not measurably affected at distances >100 μm. The spread of LTD could be described by a Gaussian function with a half-width of 56 μm (smooth curve in Fig. 6*F*). Because the region of active PFs radiates 5–10 μm from the stimulating pipette, LTD-induced changes in AMPA receptors spread $\approx$50 μm beyond the site of PF activation.

To determine the path of LTD spread, we compared the amount of LTD produced on dendritic branches where PFs were activated versus sites on other branches that were equidistant from active PF synapses. In four cells there was a 30 $\pm$ 7% reduction in glutamate responses measured along the same dendritic branch (11 sites) at distances 30–50 μm from the stimulating pipette and a 35 $\pm$ 7% change in glutamate response in other branches that were comparable distances from the stimulating pipette (six sites; not significantly different from tests along dendrite, two-tailed t test, $P = 0.3$). Thus, LTD spreads beyond the branch in which PFs are activated and may therefore spread in all directions from the site of PF activation.

Discussion

We have found that LTD of PF synapses affects AMPA-type glutamate receptors on cerebellar Purkinje cells and that these changes in AMPA receptors are quantitatively sufficient to account for the expression of LTD. Thus, expression of LTD is restricted to the postsynaptic Purkinje cell, where at least some of the signals for LTD induction are also produced (19, 26, 35, 37, 54). Our results also reveal that LTD spreads beyond active PF synapses to affect AMPA receptors on neighboring inactive synapses of the same cell, with a half-maximal range less than 60 μm.

Many of the AMPA receptors activated by uncaged glutamate should be associated with synapses that were inactive during LTD induction. Given a PF synapse density of 12–17 per micrometer length of spiny dendrite (41, 42), the 3–5 μm diameter uncaging spot encompasses $\approx$40–80 synapses along a single dendritic branch. Based on an average unitary parallel fiber synaptic response of 12 pA at -60 mV (43), we estimate that the 60-to 370-pA PF responses considered in the experiments shown in Fig. 4 were produced by the activation of only 5–30 PFs. Thus, even if all active synapses were within the uncaging spot in every experiment (and Figs. 1*E* and 2*E* indicate that may not be the case), test flashes still would activate glutamate receptors at synapses that were not active during LTD induction. Our observation that LTD equally reduces responses to PFs and to glutamate (Figs. 4 *E* and *F*; 6*A*) thus suggests that pairing can affect AMPA receptors at inactive synapses.

Although the location of active PFs was well defined in our experiments, the conclusion that LTD spreads beyond active PF synapses is independent of precise knowledge of their location. In sagittal profile, rat Purkinje cells have three to seven parallel fiber synaptic spines per μm^2 cross section of dendritic arbor (41, 42, 45), assuming 0.32–0.42 μm of dendrite per μm^2 of arbor (45). A stimulating pipette will therefore be within a 60-μm radius of 40,000–80,000 spines, if this pipette is in the center of the arbor, and somewhat fewer than half this number if the pipette is at the edge of the arbor. We estimated that 5–30 PF synapses were activated in our experiments, so that the ratio of inactive/active synapses is therefore at least 20,000/30, or 600. Thus, LTD must spread beyond active PFs to inactive PF synapses because no more than 1 of every 600 PF synapses is active within the area over which LTD is observed.

Our results are somewhat surprising given that LTD was assumed to be synapse-specific (e.g., Ref. 9). This assumption was based on observations that LTD does not spread between PF inputs separated by 100–200 μm (16) or 150–200 μm (17) and that LTD has little effect on PF synapses 40–100 μm away from the site of LTD induction (18). Our results (Fig. 6*F*) indicate that LTD should be greatly reduced at a distance of 40–100 μm and absent at 100–200 μm, which is consistent with these earlier studies. Thus, all experimental measurements of LTD are in agreement, although the spread of LTD was not detected previously because of the lower spatial resolution of earlier measurements. This does not rule out the possibility that the degree of spread in LTD may depend on experimental conditions. Our experimental conditions, namely the use of potassium rather than cesium in the patch solution (46) and the use of voltage rather than current clamp, would tend to reduce the spread of LTD by limiting depolarization due to PF activity (25).

Other relevant parameters that could affect the spread of LTD include temperature, which may affect spillover of glutamate (47) and PF stimulus intensity, which will affect the range of PF activity and resultant calcium signaling (25). Nonetheless, although the postulate of Hebb (2) has led to the widespread assumption that long-lasting synaptic plasticity is restricted to individual synapses, LTD resembles a number of other forms of plasticity that spread (4–8, 18).

Even with spatial spread, cerebellar LTD still retains a measure of associativity (Fig. 6*C*); the thousands of PF synapses affected constitute only a fraction of the 100,000–175,000 PF synapses on a Purkinje cell (33, 48, 49). This differs from the nonassociative LTD that arises from strong activity in adjacent PF synapses and appears to affect PF synapses throughout the Purkinje cell (18). Because PF synapses can be modified by competing influences from nearby synapses, LTD may couple changes in the strength of nearby but functionally disparate PF inputs. The extent to which this occurs will depend on the patterns of PF activity that occur *in vivo*. For instance, lateral spread of LTD might help coordinate multiple sensorimotor modalities. Although we have not examined this possibility, LTD also may spread between closely adjacent Purkinje cells in the way that LTP spreads between hippocampal pyramidal neurons (5).

How could LTD spread from active to inactive synapses? Diffusible messengers previously implicated in LTD include nitric oxide (NO) and cGMP (44, 50), inositol 1,4,5-trisphosphate (IP_3) (26, 51, 52), Ca^{2+} (36, 38), and glutamate (53). To account for our observations, such a chemical signal must diffuse at least 50 μm. An upper estimate of the spatial range of such signals can be derived from the time over which these signals are capable of causing LTD. The mean diffusion distance, λ, of a species with lifetime t and diffusion coefficient D, is $\lambda = \sqrt{6\ D\ t}$. For NO, a diffusion constant of 3300 $\mu m^2/s$ (54), and a coincidence requirement of 10 ms (43) yields an estimated diffusion distance of 14 μm. Assuming $t = 250$ ms (49) and D = 330 $\mu m^2/s$, the value for cAMP in molluscan neurons (55), the diffusion distance of cGMP would be 22 μm. The radius of action of IP_3 in Purkinje cell dendrites is 6 μm at resting levels of intracellular calcium (26). The range we have observed for LTD is longer than any of these distances, suggesting the involvement of even longer-range signals in LTD. One possibility is that the range of LTD is determined by the spread of downstream effectors, such as protein kinases and phosphatases (15, 56–58). Our observation that LTD spread apparently is not affected by dendritic geometry is consonant with a signal that passes through the extracellular space; of the messengers listed above, only NO and glutamate meet this requirement. Further work will be needed to understand the signaling mechanisms that allow LTD to spread from active to inactive PF synapses.

We thank our laboratory colleagues for valuable discussions, J. Eilers for comments on our manuscript, P. P. Mitra for advice on image analysis, and K. R. Gee for the gift of double-caged glutamate. This work was supported by National Institutes of Health Grant NS-34045 and fellowship NS-09457.

1. Sherrington, C. (1947) *The Integrative Action of the Nervous System,* 2nd Ed. (Yale Univ. Press, New Haven, CT).
2. Hebb, D. O. (1949) *The Organization of Behavior: A Neuropsychological Theory* (Wiley, New York).
3. Kandel, E. R. & Schwartz, J. H. (1982) *Science* **218,** 433–443.
4. Vincent, P. & Marty, A. (1993) *Neuron* **11,** 885–893.
5. Schuman, E. M. & Madison, D. V. (1994) *Science* **263,** 532–536.
6. McMahon, L. L. & Kauer, J. A. (1997) *Neuron* **18,** 295–305.
7. Engert, F. & Bonhoeffer, T. (1997) *Nature (London)* **388,** 279–284.
8. Fitzsimonds, R. M., Song, H. J. & Poo, M. M. (1997) *Nature (London)* **388,** 439–448.
9. Ito, M. (1989) *Annu. Rev. Neurosci.* **12,** 85–102.
10. Thompson, R. F. (1990) *Phil. Trans. R. Soc. London* **329,** 161–170.
11. Mauk, M. D., Garcia, K. S., Medina, J. F. & Steele, P. M. (1998) *Neuron* **20,** 359–362.
12. Lisberger, S. G. (1998) *Cell* **92,** 701–704.
13. Ito, M., Sakurai, M. & Tongroach, P. (1982) *J. Physiol. (London)* **324,** 113–134.
14. Sakurai, M. (1987) *J. Physiol. (London)* **394,** 463–480.
15. Linden, D. J. & Connor, J. A. (1995) *Annu. Rev. Neurosci.* **18,** 319–357.
16. Ekerot, C. F. & Kano, M. (1985) *Brain Res.* **342,** 357–360.
17. Kano, M. & Kato, M. (1987) *Nature (London)* **325,** 276–279.
18. Hartell, N. (1996) *Neuron* **16,** 601–610.
19. Linden, D. J., Dickinson, M. H., Smeyne, M. & Connor, J. A. (1991) *Neuron* **7,** 81–89.
20. Hemart, N., Daniel, H., Jaillard, D. & Crepel, F. (1994) *Neurosci. Res.* **19,** 213–221.
21. Pettit, D. L., Wang, S. S.-H., Gee, K. R. & Augustine, G. J. (1997) *Neuron* **19,** 465–471.
22. Edwards, F. A., Konnerth, A., Sakmann, B. & Takahashi, T. (1989) *Pflügers Arch.* **414,** 600–612.
23. Doroshenko P. A., A. Woppmann, G. Miljanich & G. J. Augustine (1997) *Neuropharmacology* **36,** 865–872.
24. Wang, S. S.-H. & Augustine, G. J. (1995) *Neuron* **15,** 755–760.
25. Eilers, J.-K., Augustine, G. J. & Konnerth, A. (1995) *Nature (London)* **373,** 155–158.
26. Finch, E. A. & Augustine, G. J. (1998) *Nature (London)* **396,** 753–756.
27. Jolliffe, I. T. (1986) *Principal Component Analysis (*Springer, New York).
28. Mitra, P. P. & Pesaran, B. (1999) *Biophys. J.* **76,** 691–708.
29. Kandler, K., Katz, L. C. & Kauer, J. A. (1998) *Nat. Neurosci.* **1,** 119–123.
30. Honore, T., Drejer, J., Fletcher, E. J., Jacobson, P., Lodge, D. & Nielson, F. E. (1988) *Science* **241,** 701–703.
31. Perkel, D. J., Hestrin, S., Sah, P. & Nicoll, R. A. (1990) *Proc. R. Soc. London B* **241,** 116–121.
32. Konnerth, A., Llano, I. & Armstrong, C. M. (1990) *Proc. Natl. Acad. Sci. USA* **87,** 2662–2665.
33. Palay, S. L. & Chan-Palay, V. (1974) *Cerebellar Cortex* (Springer, Berlin).
34. Pettit, D. L. & Augustine, G. J. (2000) *J. Neurophysiol.,* in press.
35. Takechi, H., Eilers, J. & Konnerth, A. (1998) *Nature (London)* **396,** 757–760.
36. Sakurai, M. (1990) *Proc. Natl. Acad. Sci. USA* **87,** 3383–3385.
37. Crepel, F. & Jaillard, D. (1991) *J. Physiol. (London)* **432,** 123–141.
38. Konnerth, A., Dreessen, J. & Augustine, G. J. (1992) *Proc. Natl. Acad. Sci. USA* **89,** 7051–7055.
39. Karachot, L., Kado, R. T. & Ito, M. (1994) *Neurosci. Res.* **21,** 161–168.
40. Salin, P. A., Malenka, R. C. & Nicoll, R. A. (1996) *Neuron* **16,** 797–803.
41. Napper, R. M. A. & Harvey, R. J. (1988) *J. Comp. Neurol.* **274,** 158–167.
42. Harris, K. M. & Stevens, J. K. (1988) *J. Neurosci.* **8,** 4455–4469.
43. Barbour, B. (1993) *Neuron* **11,** 759–769.
44. Lev-Ram, V., Jiang, T., Wood, J., Lawrence, D. S. & Tsien, R. Y. (1997) *Neuron* **18,** 1025–1038.
45. Berry, M. & Bradley, P. (1976) *Brain Res.* **112,** 1–35.
46. Spruston, N., Jaffe, D. B., Williams, S. H. & Johnston D. (1993) *J. Neurophysiol.* **70,** 781–802.
47. Kullmann, D. M. & Asztely, F. (1998) *Trends Neurosci.* **21,** 8–14.
48. Napper, R. M. A. & Harvey, R. J. (1988) *Comp. Neurol.* **274,** 168–177.
49. Llinas, R., Bloedel, J. R. & Hillman, D. E. (1969) *J. Neurophysiol.* **32,** 847–870.
50. Hartell, N. A. (1996) *J. Neurosci.* **16,** 2881–2890.
51. Kasono, K. & Hirano, T. (1995) *NeuroReport* **6,** 569–572.
52. Khodakhah, K. & Armstrong, C. M. (1997) *Proc. Natl. Acad. Sci. USA* **94,** 14009–14114.
53. Häusser, M. (1994) *Soc. Neurosci. Abstr.* **20,** 891.
54. Malinski, T., Taha, Z., Grunfeld, S., Patton, S., Kapturczak, M. & Tomboulian, P. (1993) *Biochem. Biophys. Res. Commun.* **193,** 1076–1082.
55. Huang, R.-C. & Gillette, R. (1991) *J. Gen. Physiol.* **98,** 835–848.
56. Ito, M. & Karachot, L. (1992) *Neurosci. Res.* **14,** 27–38.
57. Nakazawa, K., Mikawa, S., Hashikawa, T. & Ito, M. (1995) *Neuron* **15,** 697–709.
58. Boxall, A. R., Lancaster, B. & Garthwaite, J. (1996) *Neuron* **16,** 805–813.